29th EPS Conference on Plasma Phys. and Contr. Fusion Montreux, 17-21 June 2002 ECA Vol. **26B**, P-1.111 (2002)

Lattice Boltzmann Model for Dissipative MHD

Angus Macnab[1)], George Vahala[1)], Linda Vahala[2)], Pavol Pavlo[3)]

[1)] *College of William & Mary, Williamsburg, VA 23187, USA*

[2)] *Old Dominion University, Norfolk, VA 23529, USA*

[3)] *Inst. Plasma Physics, Ass. EURATOM IPP.CR, 182 21 Prague, Czech Republic*

Lattice Boltzmann Methods (LBM) provide a mesoscopic description of the transport properties of physical systems using a linearized Boltzmann equation. The benefits of these kinetic descriptions arise from the avoidance of the expensive computation present in both molecular dynamics and fluid descriptions. The benefits of LBM's are compounded by the inherent local and thus parallelizable nature of kinetic descriptions. For a particular distribution function, the linearized kinetic equation becomes:

$$\partial_t f_s + \xi_i \partial_i f_s = \frac{-1}{\tau_s}(f_s - f_s^{eq}) \tag{1}$$

where s indicates the species type and τ_s is the rate at which the distribution function f_s relaxes to f_s^{eq}. The discretized form of Eq.(1) is [1]:

$$f_a(\mathbf{x} + \mathbf{c}_a \Delta t, t + \Delta t) = (1 - \frac{1}{\tau}) f_a(\mathbf{x}, t) + \frac{1}{\tau} f_a^{eq}(\mathbf{x}, t) \tag{2}$$

We have previously shown [2, 3] that the type of lattice plays a critical role in the numerical stability of LBM's. We presently use an octagonal lattice because it possesses a higher level of isotropy than both square and hexagonal lattices.

$$\mathbf{c}_a = (\cos\frac{2\pi(a-1)}{8}, \sin\frac{2\pi(a-1)}{8}), a = 1 \ldots 8 \tag{3}$$

In choosing to connect a square grid with an octagonal streaming lattice, one must use an interpolation procedure to relate the diagonal vectors to the corresponding nodes. This is performed with a one dimensional six point Lagrange interpolation.

Equation 2 can be expanded using the standard Chapman-Enskog procedure. By using a scalar distribution function for the velocity and a vector distribution function for the magnetic field, one can recover [4, 5] the ideal MHD equations. The following definitions are needed:

density:	$\rho \equiv f_0 + \sum_a f_a^{eq}$;
momentum:	$\rho v_i \equiv \sum_a f_a^{eq} c_{a,i}$;
momentum tensor:	$\Pi_{i,j} \equiv [P + \frac{B^2}{2}]\delta_{ij} + \rho v_i v_j - B_i B_j \equiv \sum_a f_a^{eq} c_{a,i} c_{a,j}$;
magnetic field:	$B_i \equiv g_{0,i} + \sum_a g_{a,i}^{eq}$;
magnetic flux tensor:	$\Lambda_{i,j} \equiv B_i v_j - v_i B_j \equiv \sum_a g_{a,i}^{eq} c_{a,j}$.

Here, f_a^{eq} is the scalar distribution function, $g_{a,i}^{eq}$ is the vector distribution function and f_0^{eq}, $g_{0,i}^{eq}$ are the corresponding rest particle distribution functions. The relaxation

distribution functions that satisfy these definitions are:

$$f_0^{eq} = \rho - \frac{2\rho c_s^2}{c^2} - \frac{\rho}{c^2}v^2 \tag{4}$$

$$f_a^{eq} = \frac{\rho c_s^2}{4c^2} + \frac{\rho}{4c^2}v_i c_{a,i} + \frac{\rho}{2c^4}v_i v_j c_{a,i} c_{a,j} - \frac{\rho}{8c^2}v^2 - \frac{1}{2c^4}B_i B_j c_{a,i} c_{a,j} + \frac{1}{4c^2}B^2 \tag{5}$$

$$g_{0,i}^{eq} = (1-\alpha)B_i \tag{6}$$

$$g_{a,i}^{eq} = \frac{\alpha}{8}B_i + \frac{1}{4c^2}(B_i v_j c_{a,j} - v_i B_j c_{a,j}) \tag{7}$$

Where c_s is the sound speed, $P \equiv \rho c_s^2$, and α is a free parameter that affects the resistivity. The normalizing factors of c give the correct units and generalize the length of the streaming vectors. This generalized length provides explicit control of the ratio $\frac{\Delta x}{\Delta t}$ and some weighting of the negative terms which may add to the numerical instability of the model.

Upon combining the transport order terms from the Chapman-Enskog expansion with the Euler level terms, the following dissipative MHD equations are obtained:

$$\partial_t \rho + \nabla \cdot (\rho \mathbf{v}) = 0 \tag{8}$$

$$\rho \partial_t(\mathbf{v}) + \nabla(P + \frac{B^2}{2}) + \mathbf{v} \cdot \nabla \mathbf{v} = \mathbf{B} \cdot \nabla \mathbf{B} + \nu \nabla^2(\rho \mathbf{v}) + O(\nabla \cdot \mathbf{B}, \nabla^3) \tag{9}$$

$$\partial_t(\mathbf{B}) + \mathbf{B} \cdot \nabla \mathbf{v} = \mathbf{v} \cdot \nabla \mathbf{B} + \mu \nabla^2 \mathbf{B} + O(\nabla \cdot \mathbf{B}, \nabla \cdot (\rho \mathbf{v}), \nabla^3) \tag{10}$$

Where the viscosity, $\nu = \frac{1}{4}(\tau_\nu - \frac{1}{2})$ and the resistivity, $\mu = \frac{\alpha}{2}(\tau_\mu - \frac{1}{2})$ are defined by the relaxation times. The spurious $O(\nabla^3)$ terms come from higher order terms in the Chapman-Enskog expansion. The $O(\nabla \cdot \mathbf{B}, \nabla \cdot (\rho \mathbf{v}))$ terms come from numerical deviation away from divergence free $\rho \mathbf{v}$ and $\mathbf{B}$ fields.

The Biskamp-Welter vortex model [7] is a less symmetric generalization of the Orszag-Tang vortex [6]. It consists of a set of simple 2-D initial conditions which readily decay to current sheets without additional perturbations.

$$\mathbf{v}(\mathbf{x}, \mathbf{y}) = v_0 \sin(\mathbf{y} + 2.0)\hat{\mathbf{x}} - v_0 \sin(\mathbf{x} + 1.4)\hat{\mathbf{y}} \tag{11}$$

$$\mathbf{B}(\mathbf{x}, \mathbf{y}) = B_0 \sin(\mathbf{y} + 6.2)\hat{\mathbf{x}} - 2B_0 \sin(2\mathbf{x} + 2.3)\hat{\mathbf{y}} \tag{12}$$

The initial current $\mathbf{J} = \nabla \times \mathbf{B}$, and vorticity $\omega = \nabla \times \mathbf{v}$, are shown in Figure 1. We performed the simulations on a 512×512 spatial grid with periodic boundary conditions. The initial velocity and magnetic field were set to $v_0 = .150$ and $B_0 = .079$ and the initial viscosity and resistivity were set to .025 giving an initial Reynolds number of $R = 3072$ and magnetic Reynolds number of $R_m = 1618$. Approximately 543 Lattice Boltzmann time steps are equal to one of the dimensionless time steps typically used in spectral simulations. For standard Biskamp-Welter A1 conditions we obtain results similar to previous simulations [4, 7]. The phases introduced by Grauer et al. yield some interesting phenomina in our resistive MHD simulations which are not present in the corresponding ideal MHD simulations [8].

Figures (2) and (3) show the vorticity and current profiles after 1254 and 1444 LBM time steps, respectively. At $t = 1254$ the large scale initial conditions have decayed into thin current and vorticity sheets which have converged in two regions. A box like structure is visible in the center of each X point. At $t = 1444$ the box like structure has decayed through magnetic reconnection.

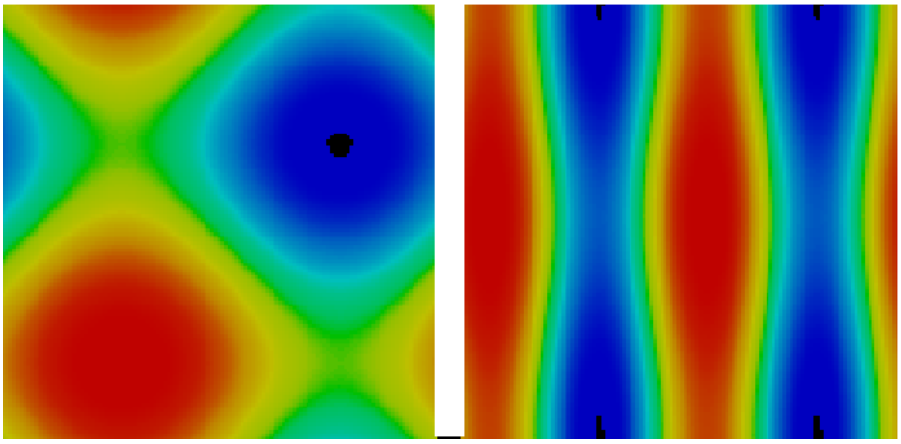

Figure 1. The vorticity(left) and current(right) at t=0. Both fields begin with large structures.

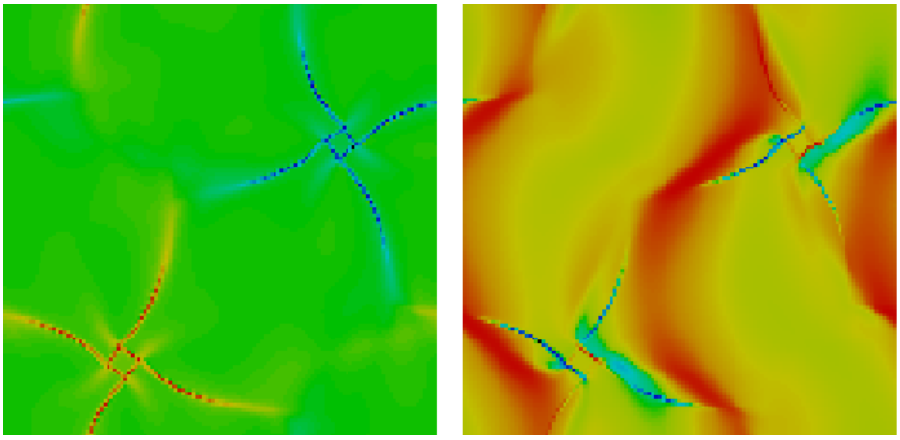

Figure 2. The vorticity(left) and current(right) at t=1254. A box structure is seen in the middle of each X point.

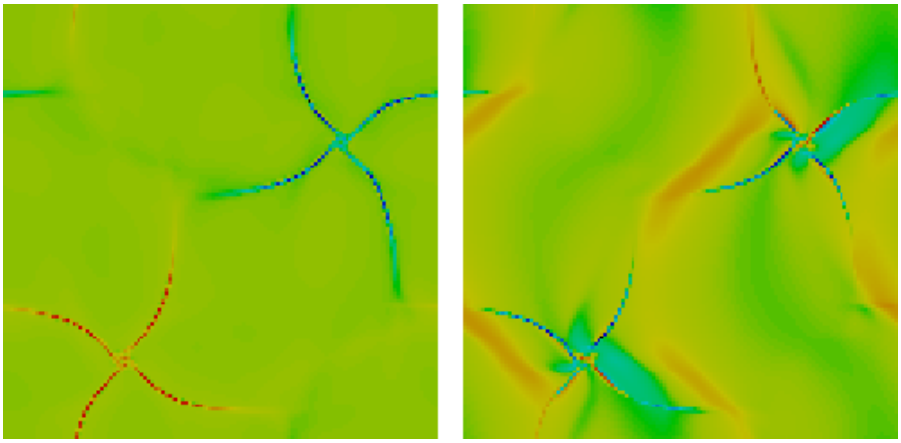

Figure 3. The vorticity(left) and current(right) at t=1444. The box structures have decayed away.

Scalar-vector LBM's represent a significant improvement over previous bi-directional streaming models because of their inherent simplicity. The increased freedom in adjusting the viscosity and resistivity along with better numerical stability make them a useful method for simulating MHD flows.

Acknowledgments

This work was supported in part by the U.S. Department of Energy and the Czech Grant Agency grant# GACR 202/00/1216.

References

[1] X. Chen, S. Chen, G. Doolen: *J. of Comp. Phys.* **146** (1998) 282.

[2] G. Vahala, P. Pavol, L. Vahala, N. Martys: *Int. J. of Mod. Phys. C* **9** (1998) 1247.

[3] A. Macnab, G. Vahala, P. Pavlo, L. Vahala, M. Soe: *28th EPS Conference on Contr. Fusion and Plasma Phys.*, Funchal, ECA **25A** (2001) 853.

[4] A. Macnab, G. Vahala, L. Vahala, P. Pavlo, M. Soe: *Czech. J. Phys.* **52**, Suppl. D (2002) D59.

[5] P. Dellar: *J. Comp. Phys.* **179** (2002) 95.

[6] S. Orszag, C. Tang: *J. Fluid Mech.* **90** (1979) 129.

[7] D. Biskamp, H. Welter: *Phys. Fluids B* **1** (1989) 1964.

[8] R. Grauer, C. Marliani: *Phys. Plasmas* **5** (1998) 2544.